Alexandria Engineering Journal (2022) 61, 4175–4188

HOSTED BY

ELSEVIER

Alexandria University

Alexandria Engineering Journal

www.elsevier.com/locate/aej
www.sciencedirect.com

Dynamics of adding variable prey refuge and an Allee effect to a predator–prey model

Hafizul Molla [a], **Sahabuddin Sarwardi** [b], **Stacey R. Smith?** [c], **Mainul Haque** [d,*]

[a] *Department of Mathematics, Manbhum Mahavidyalaya, Purulia 723 131, West Bengal, India*
[b] *Department of Mathematics & Statistics, Aliah University, IIA/27, New Town, Kolkata 700 160, West Bengal, India*
[c] *Department of Mathematics and Faculty of Medicine, The University of Ottawa, 150 Louis-Pasteur Pvt, Ottawa, ON K1N 6N5, Canada*
[d] *School of Mathematical Sciences, University of Nottingham Ningbo China, PR China*

Received 28 June 2021; revised 30 August 2021; accepted 14 September 2021
Available online 01 October 2021

KEYWORDS

Ecological model;
Refuge;
Permanence;
Stability;
Bifurcations;
Hopf bifurcation

Abstract Prey refuge from predators can play an important role in stabilising an ecological system by reducing interactions between species, while Allee effects can arise from a range of biological phenomena, such as anti-predator vigilance, genetic trends and feeding deficiencies. We develop a predator–prey model that combines these phenomena, considering variable prey refuge with additive Allee effect on the prey species, with a Holling type II response function for the prey growth function. We use the predator and prey nullclines to determine the existence and stability of interior equilibria. We also investigate all possible local and global bifurcations that the system could undergo, showing that prey refuge and a strong Allee effect can lead to saddle-node bifurcations, Hopf bifurcations or Bogdanov–Takens bifurcation. We have investigated the appearance of Hopf bifurcations in a neighborhood of the unique interior equilibrium point of the dynamical system. The rich behaviour of the dynamics suggests that both prey refuge and a strong Allee affect are important factors in ecological complexity.

1. Introduction

The dynamical relationship between prey and their predators is one of the dominant themes in ecology due to its universal existence and importance [25], with predator–prey interaction one of the most extensively studied issues in the ecological and mathematical literature [24].

Ecological models are often used to simulate the dynamics of a system of interacting populations. Lotka [13] and Volterra [40] proposed the classical predator–prey models, which represent the basis of mathematical ecology. Numerous mathematical models have been developed according to the framework of the pioneering work of Lotka and Volterra. In a predator–prey model, the functional response represents the prey consumption rate by a predator. Besides the response function, many other factors influence the dynamics [44] of interaction,

* Corresponding author.
E-mail address: mainul.mainul@gmail.com (M. Haque).
Peer review under responsibility of Faculty of Engineering, Alexandria University.

https://doi.org/10.1016/j.aej.2021.09.039

such as prey refuge [18,39], harvesting [15], sickness and the Allee effect [38,33,45,16,6,46].

Prey refuge plays an important role in stabilizing an ecological system by reducing the encounter rate between predator and prey. Two types of refuge are standard: one for which the amount of refuge is proportional to the prey volume, with the remaining prey available for predation. In the other, the prey refuge is a fixed quantity. In case of constant refuge, the stable Lotka–Volterra dynamical system is not affected. However, an extensive refuge replaces the limit cycles with a stable equilibrium [9,34].

Generally, the effects of prey refuge (cf. Saha et al. [27]) on the interacting population dynamics [41,29] are considered via a predator–prey model [28,12] incorporating a constant proportion of prey refuge with a Holling type II response function [10,11,43]. We also investigate the population outcomes of refuge used in the Lotka–Volterra model comprising self restriction when refuge is proportional to the interactions between predator and prey.

In addition, the Allee effect may appear due to an extensive range of biological phenomena, like reduced anti-predator vigilance, genetic trends, mating difficulty and feeding deficiency at low population densities [3,19]. Pal and Mandal [20] analyzed a modified Leslie–Gower predator–prey model where the growth function of prey population was governed by a multiplicative strong Allee effect, with a Beddington–DeAngelis response functional [22,21]. Cai et al. [4] analyzed a modified Leslie–Gower predator–prey model with additive Allee effect using a Holling type II functional response. One of their most interesting findings is that the Allee effect can increase the risk of ecological extinction. Thus, the combined impact of Allee effects and prey refuge on population dynamics of predator–prey interactions may lead to a better understanding of conditions that may lead to species extinction. Consequently, we consider a predator–prey model with Holling type II functional response and an additive Allee effect on the prey growth function.

Our paper is organized as follows: In Section 2, we develop the baseline model and add the Allee effect and refuge. In Section 3, we present preliminary results, such as equilibria, boundedness, persistent and permanent of the system. In Section 4, we determine the local stability of each of the equilibria. In Section 5, we established criteria for local and global bifurcations using center-manifold and normal-form theory. In Section 6, we illustrate our theoretical results with numerical simulations. Finally, in Section 7, we discuss the implications of our results.

2. Model formulation

We develop a modified Lotka–Volterra model with self-limitating growth. We first consider refuge to be directly proportional to the interaction between predator and prey. Let $x(t)$ and $y(t)$ be the prey and predator populations, respectively, with x_r the amount of refuge admissible for $t \geqslant 0$ with $0 \leqslant (x - x_r) \leqslant x$. We use the Holling type II response function $\frac{mx}{a+x}$ to model the effect of predator saturation, which is experienced when a large volume of prey are available [5,36]. During the interaction between predator and prey, some prey can escape from predation. Taking into account the refuge function determined by $x_r = \delta xy$, our baseline model is as follows:

$$\frac{dx}{dt} = rx\left(1 - \frac{x}{K}\right) - \frac{m(x - x_r)y}{a + (x - x_r)}, \tag{2.1a}$$

$$\frac{dy}{dt} = \left(\frac{em(x - x_r)}{a + (x - x_r)} - d\right)y. \tag{2.1b}$$

Next, we incorporate an additive Allee effect term $\frac{n}{x+h}$, extending model (2.1) to

$$\frac{dx}{dt} = rx\left(1 - \frac{x}{K} - \frac{n}{x + h}\right) - \frac{mx(1 - \delta y)y}{a + x(1 - \delta y)}, \tag{2.2a}$$

$$\frac{dy}{dt} = \left(\frac{emx(1 - \delta y)}{a + x(1 - \delta y)} - d\right)y, \tag{2.2b}$$

where r is the intrinsic growth rate of the prey, K is the carrying capacity, m is the prey consumption rate by the predator, δ is the coefficient of prey refuge, a is the half-saturation constant of the prey, e is the conversion efficiency and d is the natural mortality rate of the predator. Finally, n and h describe the degree of the Allee effect. For ecological realism, we restrict δ such that $(1 - \delta y) \geqslant 0$ [17,8].

The Allee effect is strong if the condition $0 < h < n$ holds; if the condition $0 < n < h$ holds, then it is a weak Allee effect. Biologically, a strong Allee effect implies that losses from the undercrowding at low levels outweigh gains; a weak Allee efect does not have this requirement [7]. We chose to use the additive term $\frac{n}{x+h}$ as it is the simplest form that gives both a strong and weak Allee effect.

3. Preliminary analysis

3.1. Invariance of the domain Ω of the system (2.2)

The set $\Omega = \{(x, y) \in \mathbb{R}^2_+ : 0 \leqslant x \leqslant K, 0 \leqslant y \leqslant \frac{1}{\delta}\}$ is invariant in the region Ω. Assuming $(1 - \delta y) > 0$, then $\frac{dx}{dt} = \frac{-mx(1-\delta y)y}{a+x(1-\delta y)} < 0$ at $x = K$and $\frac{dy}{dt} = \frac{-d}{\delta} < 0$ when $y = \frac{1}{\delta}$. Hence the trajectories cross into the interior of Ω. The axes $x = 0, y = 0$ are invariant. In addition, the set $\Omega = \{(x, y) \in \mathbb{R}^2_+ : 0 \leqslant x \leqslant K, 0 \leqslant y \leqslant \frac{1}{\delta}\}$ is compact and invariant.

3.2. Uniform boundedness

To show that the system is uniformly bounded, we define $\Lambda = x + \frac{1}{e}y$ for $0 < e < 1$. If we choose $d > p > 0$, then the following inequalities hold:

$$\begin{aligned}\frac{d\Lambda}{dt} + p\Lambda &= rx\left(1 - \frac{x}{K} - \frac{n}{x + h}\right) - \frac{dy}{e} + px + \frac{py}{e} \\ &\leqslant \frac{r}{K}\left\{\frac{(r + p)K}{r} - x\right\}x \leqslant \frac{K(r + p)^2}{4r} \equiv \phi.\end{aligned}$$

Since $x \leqslant K$, by differential inequality theory [2], we can write

$$0 < \Lambda(x, y) < \frac{\phi(1 - e^{-pt})}{p} + \Lambda(x(0), y(0))e^{-pt}.$$

When $t \to \infty$, we have $0 < \Lambda < \frac{\phi}{p}$. Then all solutions of (2.2) that start in $\mathbb{R}^2_+$ are enclosed in the domain $\Omega = \left\{(x, y) \in \mathbb{R}^2_+ : \Lambda = \frac{\phi}{p} + \epsilon\right\}$, where ϵ is a small positive quantity.

3.3. Feasible equilibria

The following conditions hold for system (2.2)

(a) The trivial equilibrium $E_0 = (0,0)$ is always feasible.
(b) The axial equilibria are $E^{\pm} = (x^{\pm}, 0)$, where $x^{\pm} = \frac{(K-h)\pm\sqrt{(K-h)^2-4K(n-h)}}{2}$. $E^{\pm}$ are feasible if $K > h$ and $(K+h)^2 > 4Kn$.
(c) The interior equilibrium point $E^* = (x^*, y^*)$ is feasible if $em > d$ and $x^* > \frac{ad}{em-d}$ hold, where $y^* = \frac{(em-d)x^*-ad}{\delta(em-d)x^*}$ and x^* is the root of the equation

$$A_4X^4 + A_3X^3 + A_2X^2 + A_1X + A_0 = 0,$$

where

$$\begin{aligned} A_4 &= -\delta er(em-d),\\ A_3 &= K\delta e^2mr - \delta e^2hmr - Kd\delta er + d\delta ehr,\\ A_2 &= K\delta e^2hmr - K\delta e^2mnr - Kd\delta ehr + Kd\delta enr - medK + Kd^2,\\ A_1 &= -Kdehm + Kad^2 + Kd^2h,\\ A_0 &= Kad^2h. \end{aligned}$$

It is very difficult to define parametric conditions for the existence of the actual number of coexistence equilibrium points, though the possible number of positive coexistence equilibrium points can be described through the comparative positions of the non-trivial nullclines; i.e., $\frac{1}{x}\frac{dx}{dt} = 0$ and $\frac{1}{y}\frac{dy}{dt} = 0$ as presented in Fig. 1.

3.4. Persistence

Proposition 1. *The system is persistent for the weak Allee effect if (i) $r(h-n) > dh$ and (ii) $x^{\pm} > \frac{ad}{em-d}$ are satisfied.*

Proof. Consider a Lyapunov function $V(x,y) = xy$. Then

$$\begin{aligned} \Delta(x,y) &= \frac{\dot{V}(x,y)}{V(x,y)} = \frac{\dot{x}}{x} + \frac{\dot{y}}{y}\\ &= r\left(1 - \frac{x}{K} - \frac{n}{x+h}\right) + \frac{m(1-\delta y)}{a + x(1-\delta y)}(ex - y) - d. \end{aligned}$$

For the weak Allee effect ($n < h$), the mean individual fitness of a population is reduced but always positive at lower population volumes. The value of Δ at the trivial equilibrium point is $\Delta(0,0) = r(1-\frac{n}{h}) - d > 0$ if the condition $r(h-n) > dh$ holds.

For the axial equilibria $(x^{\pm}, 0)$, we have

$$\Delta(x^{\pm}, 0) = \frac{emx^{\pm}}{a + x^{\pm}} - d > 0,$$

if $x^{\pm} > \frac{ad}{em-d}$. Hence the system is persistent for the weak Allee effect.

Note: For the strong Allee effect ($n > h$), we have $\Delta(0,0) < 0$, so there exist a critical population volume under which the mean individual fitness of a population is negative and the population will go extinct.

3.5. Permanence

Proposition 2. *The system is permanent if the condition $K\{1 - (\frac{m}{a\delta r} + \frac{n}{h})\} > 0$ holds.*

Proof. We can choose $x(t) \leqslant K$ for all $t > 0$ and, from (2.2b), we can write

$$\frac{dy}{dt} \leqslant \left(\frac{emx(1-\delta y)}{a + x(1-\delta y)}\right)y \leqslant \frac{kem(1-\delta y)y}{a} \leqslant \frac{kem\delta}{a}\left(\frac{1}{\delta} - y\right)y.$$

It can be easily shown that

$$\limsup_{t\to\infty} y(t) \leqslant \frac{1}{\delta}.$$

From (2.2a), we have

$$\begin{aligned} \frac{dx}{dt} &= rx\left(1 - \frac{x}{K} - \frac{n}{x+h}\right) - \frac{mx(1-\delta y)y}{a + x(1-\delta y)}\\ &\geqslant \frac{rx}{k}\left\{K\left(1 - \left(\frac{m}{a\delta r} + \frac{n}{h}\right)\right) - x\right\}\\ &\geqslant \frac{rx}{k}(x' - x), \end{aligned}$$

where $x' = K\left(1 - \left(\frac{m}{a\delta r} + \frac{n}{h}\right)\right) > 0$. Using (2.2b), we have

$$\frac{dy}{dt} = \left(\frac{emx(1-\delta y)}{a + x(1-\delta y)}\right)y \geqslant \frac{em\delta x'}{a+k}y(y' - y),$$

where $y' = \frac{emx' - d(a+k)}{\delta emx'} > 0$. Choosing a small positive quantity ϵ satisfying $\epsilon < \min(x', y')$, it can be concluded that

$$\liminf_{t\to\infty} x(t) > \epsilon \text{ and } \liminf_{t\to\infty} y(t) > \epsilon.$$

4. Stability analysis

We have the following results:

(i) The eigenvalues of the Jacobian matrix J (see Appendix A.1) at $E_0 = (0,0)$ are $-\frac{r(n-h)}{h}$ and $-d$. Therefore, the trivial equilibrium point $E_0 = (0,0)$ is locally asymptotically stable if $n > h$ (strong Allee effect) and unstable if $n < h$ (weak Allee effect).
(ii) The axial equilibrium points $E^{\pm} = (x^{\pm}, 0)$ are locally asymptotically stable if

$$x^{\pm} < \frac{ad}{em-d}$$

and

$$x^{\pm 3} + (-K/2 + 2h)x^{\pm 2} - h(K-h)x^{\pm} + 1/2\,Kh(n-h) > 0.$$

(iii) Evaluating the Jacobian matrix at the interior equilibrium point $E^* = (x^*, y^*)$, system (2.2) is locally asymptotically stable if the condition

$$\delta < \min\left(\frac{Kemdx^*(x^*+h)^2(em-d)}{\delta_1}, \frac{\delta_2}{\delta_3}\right)$$

is satisfied, where the values of δ_1, δ_2 and δ_3 are given in Appendix A.2.

The stability conditions for all equilibria are detailed in Table 1.

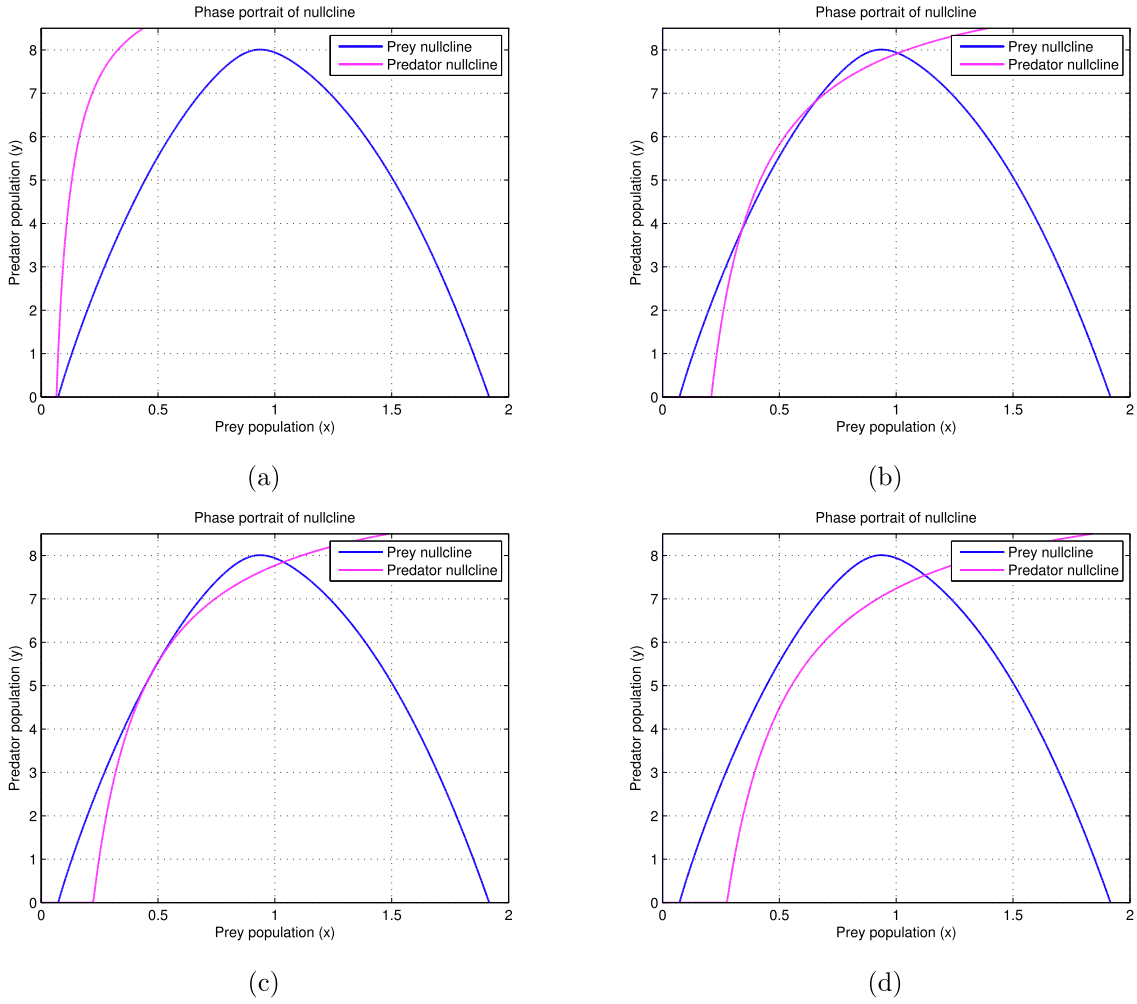

Fig. 1 Possible number of positive interior equilibrium points for different values of the predator mortality rate d. (a) No interior equilibrium point in the feasible region for $d = 0.0035$. (b) Three equilibria for $d = 0.00446$. (c) There exist two equilibria for the predator mortality rate $d = 0.004495$. (d) There exists only one equilibrium point for $d = 0.0046$. The other parameters are as follows: $K = 2$, $\delta = 0.1$, r = 0.28, n = 0.08, h = 0.01, m = 0.017, a = 0.03 and $e = 0.3$.

Table 1 Schematic presentation of analytical findings at all equilibrium points. LAS = locally asymptotically stable, SN = saddle-node bifurcation, HB = Hopf bifurcation.

Equilibria	Existence condition	Necessary condition	Nature
E_0	–	$n > h$	LAS
E^+	$K > h$, $(K+h)^2 > 4Kn$	$x^+ < \frac{ad}{(em-d)}$	LAS
E^-	$n > h$	$x^- < \frac{ad}{(em-d)}$	LAS
E^*	$x^* > \frac{ad}{(em-d)}$	$\delta < \min\left(\frac{Kdemx^*(x^*+h)^2(em-d)}{\delta_1}, \frac{\delta_2}{\delta_3}\right)$	LAS
E^*	$x^* > \frac{ad}{(em-d)}$	$\delta_{sn} = 0.1015$	SN
E^*	$x^* > \frac{ad}{(em-d)}$	$\delta_{hb} = 0.0927$	HB

5. Bifurcation analysis

5.1. Saddle-node bifurcation

Evaluating the Jacobian matrix of the model system (2.2) at the interior equilibrium point $E^* = (x^*, y^*)$, we have

$$J^* = \begin{bmatrix} a_{11} & a_{12} \\ a_{21} & a_{22} \end{bmatrix}_{(x^*, y^*, \delta_{sn})},$$

where

$$a_{11} = rx^*\left(\frac{1}{K} + \frac{n}{(x^*+h)^2}\right) + \frac{d^2 y^*}{e^2 m x^*}, \quad a_{12} = \frac{(y^*(-2em+d)\delta + em)d}{e^2 m(\delta y^* - 1)},$$
$$a_{21} = \frac{d(em-d)y^*}{emx^*}, \quad a_{22} = \frac{\delta d(d - emx^*)y^*}{emx^*(1 - \delta y^*)}.$$

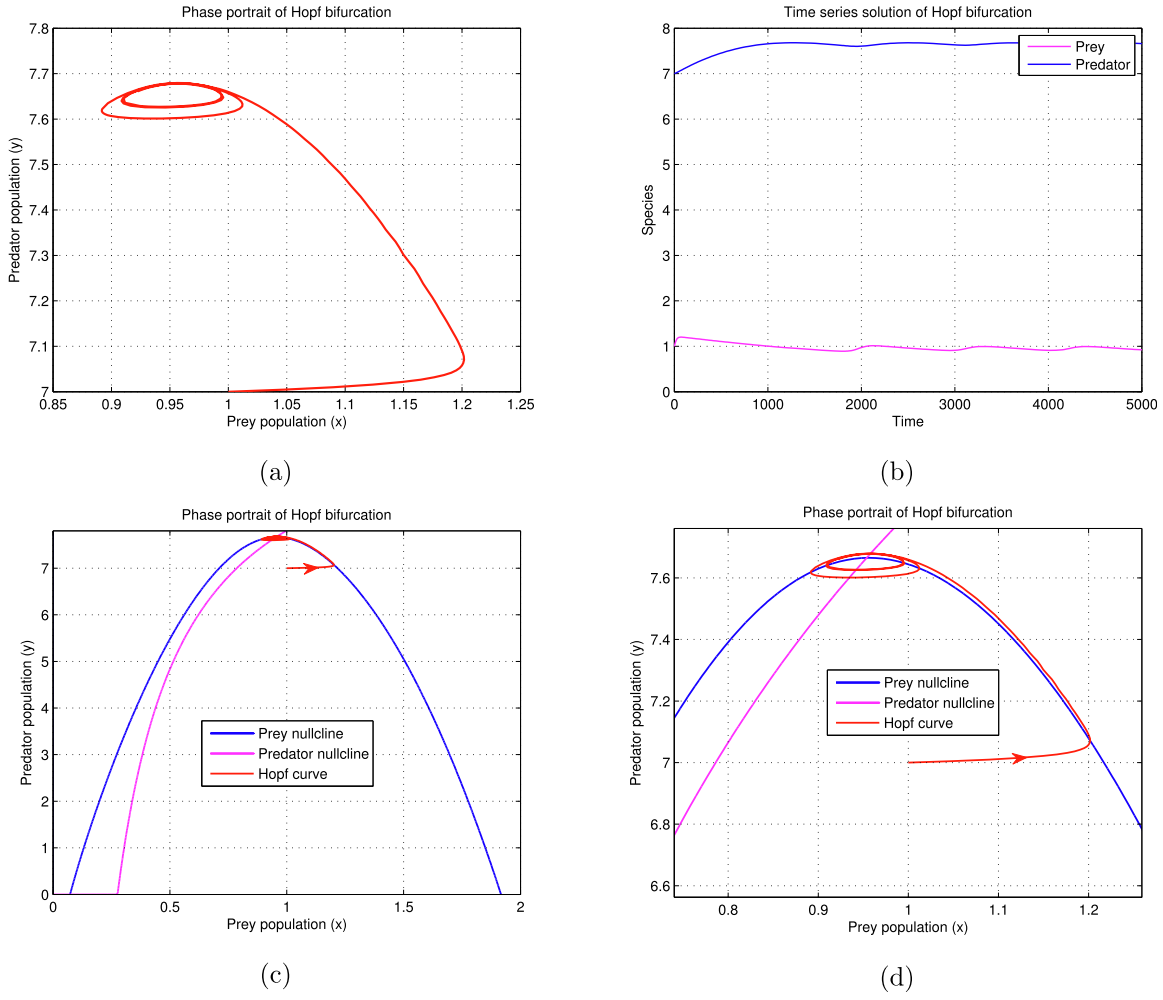

Fig. 2 (a) Phase portrait of Hopf bifurcation around the unique coexistence equilibrium point $(0.9519699, 7.663688)$ for threshold value of refuge coefficient $\delta_{hb} = 0.0927$. (b) Time series solution of Hopf bifurcation, (c) Phase portrait of Hopf bifurcation with predator and prey nullclines. (d) Macro figure of $2(c)$. All other parameters are given in Table 2.

For the set of parameters $K = 2$, r = 0.28, n = 0.08, h = 0.01, m = 0.017, a = 0.03, e = 0.3 and $d = 0.0042$, one of the eigenvalues of J^* vanishes if and only if $\det(J^*)|_{E^*} = 0$, which gives the threshold value $\delta = \delta_{sn} = \frac{\eta_1}{\eta_2} = 0.1015$, where

$$\begin{aligned}\eta_1 &= Kdemx^*(x^*+h)^2(em-d),\\ \eta_2 &= Ke^3m^2nrx^{*3} - e^3h^2m^2rx^{*3} - 2e^3hm^2rx^{*4} - e^3m^2rx^{*5}\\ &\quad +2Kde^2h^2m^2x^*y^* + 4Kde^2hm^2x^{*2}y^* + 2Kde^2m^2x^{*3}y^*\\ &\quad -2Kd^2eh^2mx^*y^* - 4Kd^2ehmx^{*2}y^* - 2Kd^2emx^{*3}y^*\\ &\quad -Kde^2mnrx^{*2} + de^2h^2mrx^{*2} + 2de^2hmrx^{*3} + de^2mrx^{*4}\\ &\quad +Kd^3h^2x^*y^* + 2Kd^3hx^{*2}y^* + Kd^3x^{*3}y^* - Kd^3h^2y^*\\ &\quad -2Kd^3hx^*y^* - Kd^3x^{*2}y^*.\end{aligned}$$

The other eigenvalue is $\mathrm{tr}(J^*)$ evaluated at $\delta = \delta_{sn}$. The eigenvectors corresponding to zero eigenvalues of the Jacobian matrix J^* and its transpose are $v_1 = \left(\frac{\delta(-emx^*+d)}{(\delta y^*-1)(em-d)}, 1\right)^T$ and $v_2 = \left(\frac{ey^*\delta(-emx^*+d)}{x^*(y^*(-2em+d)\delta+em)}, 1\right)^T$, respectively. Denote model (2.2) by $(x\prime, y\prime)^T = (F_1(x,y), F_2(x,y))^T \equiv F(x,y)$. We have $F_\delta = \frac{\partial F}{\partial \delta}$ and $DF_\delta = \frac{\partial (DF)}{\partial \delta}$. Denoting the eigenvector $\xi = (\xi_1, \xi_2)^T$ corresponding to the matrix J^* [26], one can define the quantities $F_\delta(E^*, \delta_{sn})$ and $D^2F(E^*, \delta_{sn})(\xi, \xi)$. We thus have $v_2^T[F_\delta(E^*, \delta_{sn})] = -\frac{emy^{*2}a(-\delta_{sn}emx^*y^*+d\delta_{sn}x^*y^*-d\delta_{sn}y^*+emx^*)}{(-\delta_{sn}x^*y^*+a+x^*)^2(-2\delta_{sn}emy^*+d\delta_{sn}y^*+em)} = -8.5977 \neq 0$. Therefore, system (2.2) attains neither a transcritical nor a pitchfork bifurcation under the given parametric restriction. Since the value of the expression

$$v_2^T[D^2F(E^*, \delta_{sn})(v_1, v_1)] = 0.1335 \neq 0,$$

by Sotomayor's theorem [37], system (2.2) undergoes a non-degenerate saddle-node bifurcation of co-dimension one around the interior equilibrium point $E^* = (x^*, y^*) = (0.9153, 8.3456)$ when δ pass through its threshold value $\delta_{sn} = 0.1015$.

5.2. Hopf bifurcation

We define the critical value of the bifurcation parameter $\delta = \delta_{hb}$ as $\mathrm{tr}(J^*)|_{\delta=\delta_{hb}} = 0$ and $\det(J^*)|_{\delta=\delta_{hb}} \neq 0$ around the interior equilibrium point (x^*, y^*). To ensure the existence of a Hopf bifurcation around the coexistence equilibrium point $(0.9520, 7.6637)$, we have to verify the transversality condition for the critical value of $\delta = \delta_{hb} = 0.0927$. We have $\left[\frac{d}{d\delta}\mathrm{tr}(J^*)\right]_{\delta=\delta_{hb}} = \frac{d(-emx^*+d)y^*}{emx^*(\delta_{hb}y^*-1)} = -0.0220 \neq 0$ for the parametric

values $K=2$, $\delta_{hb}=0.0927$, $r=0.28$, $n=0.08$, $h=0.01$, $m=0.017$, $a=0.03$, $e=0.3$ and $d=0.0046$. Hence the stability of the dynamical system can change at the interior equilibrium point $(x^*,y^*)=(0.9520,7.6637)$ through a Hopf bifurcation.

We can calculate the Lyapunov number to determine the nature of periodic solutions of the Hopf bifurcation. Taking a small perturbation $x=(x_1+x_\delta)|_{\delta=\delta_{hb}}$ and $y=(y_1+y_\delta)|_{\delta=\delta_{hb}}$ and using Taylor series expansions of equation (2.2), we have

$$\begin{aligned}\dot{x_1} &= p_{10}x_1+p_{01}y_1+p_{20}x_1^2+p_{11}x_1y_1+p_{02}y_1^2+\cdots,\\ \dot{y_1} &= q_{10}x_1+q_{01}y_1+q_{20}x_1^2+q_{11}x_1y_1+q_{02}y_1^2+\cdots,\end{aligned}$$

where p_{10},p_{01},q_{10} and q_{01} represent the elements of the Jacobian matrix at the coexistence equilibrium point $E^*=(x^*,y^*)$ with the threshold value δ_{hb}. Therefore $p_{10}+q_{01}=0$ and $\Delta=(p_{10}q_{01}-p_{01}q_{10})>0$. The expression $p_{ij}=\frac{1}{i!j!}\frac{\partial^{(i+j)}F_1}{\partial x^i\partial y^j}|_{(E^*,\delta_{hb})}$ and $q_{ij}=\frac{1}{i!j!}\frac{\partial^{(i+j)}F_2}{\partial x^i\partial y^j}|_{(E^*,\delta_{hb})}$, where $i,j=0,1,2,3$ (neglecting higher order terms) are as follows:

$$\begin{aligned}&p_{10}=\frac{\partial F_1}{\partial x}|_{(E^*,\delta_{hb})},\quad p_{01}=\frac{\partial F_1}{\partial y}|_{(E^*,\delta_{hb})},\quad p_{12}=\frac{1}{2}\frac{\partial^3F_1}{\partial x\partial y^2}|_{(E^*,\delta_{hb})},\\ &p_{21}=\frac{1}{2}\frac{\partial^3F_1}{\partial x^2\partial y}|_{(E^*,\delta_{hb})},\quad p_{20}=\frac{1}{2}\frac{\partial^2F_1}{\partial x^2}|_{(E^*,\delta_{hb})},\quad p_{11}=\frac{\partial^2F_1}{\partial x\partial y}|_{(E^*,\delta_{hb})},\\ &p_{30}=\frac{1}{6}\frac{\partial^3F_1}{\partial x^3}|_{(E^*,\delta_{hb})};\quad q_{10}=\frac{\partial F_2}{\partial x}|_{(E^*,\delta_{hb})},\quad q_{01}=\frac{\partial F_2}{\partial y}|_{(E^*,\delta_{hb})},\\ &q_{12}=\frac{1}{2}\frac{\partial^2F_2}{\partial x\partial y^2}|_{(E^*,\delta_{hb})},\quad q_{21}=\frac{1}{2}\frac{\partial^3F_2}{\partial x^2\partial y}|_{(E^*,\delta_{hb})},\quad q_{20}=\frac{1}{2}\frac{\partial^2F_2}{\partial x^2}|_{(E^*,\delta_{hb})},\\ &q_{11}=\frac{\partial^2F_2}{\partial x\partial y}|_{(E^*,\delta_{hb})},\quad q_{03}=\frac{1}{6}\frac{\partial^3F_2}{\partial y^3}|_{(E^*,\delta_{hb})}.\end{aligned}$$

Details of the expressions $p_{i,j}$ and $q_{i,j}$, $(i,j=0,1,2,3.)$ are given in the Appendix A.3.

The value of the first Lyapunov number η [23] describes the nature of the periodic solution occurring through the Hopf bifurcation and is given by

$$\begin{aligned}\eta = &-\frac{3\pi}{2p_{01}\Delta^{\frac{3}{2}}}[\{p_{10}q_{10}(p_{11}^2+p_{11}q_{02}+p_{02}q_{11})+p_{10}a_{01}(q_{11}^2+p_{20}q_{11}+p_{11}q_{02})\\ &+q_{10}^2(p_{11}p_{02}+2p_{02}q_{02})-2p_{10}q_{10}(q_{02}^2-p_{20}p_{02})-2p_{10}p_{01}(p_{20}^2-q_{20}q_{02})\\ &-p_{01}^2(2p_{20}q_{20}+q_{11}q_{20})+(p_{01}q_{10}-2p_{10}^2)(q_{11}q_{02}-p_{11}p_{20})\}\\ &-(p_{10}^2+p_{01}q_{10})\{3(q_{10}q_{03}-p_{01}p_{30})+2p_{10}(p_{21}+q_{12})+(q_{10}p_{12}-p_{01}q_{21})\}].\end{aligned}$$

The periodic solution is subcritical or supercritical in nature if the value of $\eta>0$ or $\eta<0$, respectively [1]. According to our given parametric restriction (see Fig. 2) the numerical value of the first Lyapunov number η is $484.6445>0$. Therefore, the nature of the periodic solution of the dynamical system (2.2) undergoes a subcritical Hopf bifurcation.

5.3. Bogdanov–Takens bifurcation

Next we examine the Bogdanov–Takens bifurcation of (2.2) in a small neighborhood of $E^*=(x^*,y^*)$. There exists a degenerate interior equilibrium point for a given parametric restriction in which both the eigenvalues of the Jacobian matrix vanish. Applying a series of nontrivial coordinate transformations, we have to transform system (2.2) to its canonical form. Considering δ and r as Bogdanov–Takens bifurcation parameters, we can shift the interior equilibrium point (x^*,y^*) to the origin by making a coordinate transformation $x=x^*+x_1$, $y=y^*+y_1$. With the help of a Taylor series expansion, (2.2) is transformed as follows:

$$\frac{dx_1}{dt}=c_{10}x_1+c_{01}x_2+c_{11}x_1^2+c_{12}x_1x_2+c_{22}x_2^2+O(\|x\|^3), \quad (5.1a)$$

$$\frac{dx_2}{dt}=d_{10}x_1+d_{01}x_2+d_{11}x_1^2+d_{12}x_1x_2+d_{22}x_2^2+O(\|x\|^3), \quad (5.1b)$$

where

$$\begin{aligned}&c_{10}=\frac{\partial F_1}{\partial x}|_{(x^*,y^*)},\quad c_{01}=\frac{\partial F_1}{\partial y}|_{(x^*,y^*)},d_{10}=\frac{\partial F_2}{\partial x}|_{(x^*,y^*)},\\ &d_{01}=\frac{\partial F_2}{\partial y}|_{(x^*,y^*)},\quad c_{11}=\frac{1}{2}\frac{\partial^2F_1}{\partial x^2}|_{(x^*,y^*)},\quad c_{12}=\frac{\partial^2F_1}{\partial x\partial y}|_{(x^*,y^*)},\\ &c_{22}=\frac{1}{2}\frac{\partial^2F_1}{\partial y^2}|_{(x^*,y^*)},\quad d_{11}=\frac{1}{2}\frac{\partial^2F_2}{\partial x^2}|_{(x^*,y^*)},\quad d_{12}=\frac{\partial^2F_2}{\partial x\partial y}|_{(x^*,y^*)},\\ &d_{22}=\frac{1}{2}\frac{\partial^2F_2}{\partial y^2}|_{(x^*,y^*)},\end{aligned}$$

satisfying the conditions $(c_{10}+d_{01})=0$ and $(c_{10}d_{01}-c_{01}d_{10})=0$. For details of the above coefficients, see Appendix A.4.

Introducing another transformation $y_1=x_1$, $y_2=px_1+qx_2$, (5.1) transforms to

$$\frac{dy_1}{dt}=y_2+c_{11}^1y_1^2+c_{12}^1y_1y_2+c_{22}^1y_2^2+O(\|y\|^3), \quad (5.2a)$$

$$\frac{dy_2}{dt}=d_{11}^1y_1^2+d_{12}^1y_1y_2+d_{22}^1y_2^2+O(\|y\|^3), \quad (5.2b)$$

where

$$\begin{aligned}c_{11}^1 &= \tfrac{c_{22}c_{10}^2}{c_{01}^2}-\tfrac{c_{12}c_{10}}{c_{01}}+c_{11},\quad c_{12}^1=-\tfrac{2c_{22}c_{10}}{c_{01}^2}+\tfrac{c_{12}}{c_{01}},\\ c_{22}^1 &= \tfrac{c_{22}}{c_{01}^2},\quad d_{11}^1=c_{11}c_{01}+(c_{11}-d_{11})c_{10}-\tfrac{(c_{12}-d_{22})c_{10}^2}{c_{01}}+\tfrac{c_{22}c_{10}^3}{c_{01}^2},\\ d_{12}^1 &= -\left[\tfrac{2c_{22}c_{10}^2}{c_{01}^2}-\tfrac{(c_{12}-2d_{22})}{c_{01}}-d_{12}\right],\quad d_{22}^1=\tfrac{c_{22}c_{10}}{c_{01}^2}+\tfrac{d_{22}}{c_{01}}.\end{aligned}$$

Applying a C^∞ invertible transformation

$$\begin{aligned}z_1 &= y_1+\tfrac{1}{2}\left(\tfrac{c_{11}c_{10}}{c_{01}^2}-\tfrac{(c_{12}+d_{22})}{c_{01}}\right)y_1^2-\tfrac{c_{22}}{c_{01}^2}y_1y_2,\\ z_2 &= y_2-\left(\tfrac{c_{11}c_{10}}{c_{01}^2}+\tfrac{d_{22}}{c_{01}}\right)y_1y_2+\left(\tfrac{c_{22}c_{10}^2}{c_{01}^2}-\tfrac{c_{12}c_{10}}{c_{01}}+c_{11}\right)y_1^2,\end{aligned}$$

Eq. (5.2) reduces to

$$\frac{dz_1}{dt}=z_2+O(\|z\|^3), \quad (5.3a)$$

$$\frac{dz_2}{dt}=\beta_1z_1^2+\beta_2z_1z_2+O(\|z\|^3), \quad (5.3b)$$

where $\beta_1=c_{11}c_{01}+(c_{11}-d_{11})c_{10}-\frac{(c_{12}-d_{22})c_{10}^2}{c_{01}}+\frac{c_{22}c_{10}^3}{c_{01}^2}$ and $\beta_2=-\frac{c_{10}}{c_{01}}(c_{12}+2d_{22})+2c_{11}+d_{12}$.

For the transformation

$$\begin{aligned}w_1 &= z_1,\\ w_2 &= z_2+O(\|z\|^3),\end{aligned}$$

Eq. (5.3) can be transformed as follows:

$$\frac{dw_1}{dt}=w_2 \quad (5.4a)$$

$$\frac{dw_2}{dt}=\beta_1w_1^2+\beta_2w_1w_2+O(\|z\|^3). \quad (5.4b)$$

Rescaling according to Wiggins [42], we write $w_1=\bar{\beta}_1w_1$, $w_2=\bar{\beta}_2w_2$ and $t=\tau t$ (with $\tau>0$). Neglecting higher-order terms, system (5.4) transforms to

$$\frac{dw_1}{dt}=\eta_1w_2 \quad (5.5a)$$

$$\frac{dw_2}{dt}=\eta_2w_1^2+\rho w_1w_2, \quad (5.5b)$$

where $\eta_1 = \frac{\tau\bar{\beta}_2}{\bar{\beta}_1}, \eta_2 = \frac{\tau\beta_1\bar{\beta}_2{}^2}{\bar{\beta}_2}$ and $\rho = \tau\bar{\beta}_1\beta_2$. Moreover, we have to choose values of $\bar{\beta}_2, \bar{\beta}_2$and τ in such a way that the values of η_1, η_2 and ρ are constrained to the identity. If we choose the value of $\eta_1 = 1$, then it can be easily found that $\tau = \frac{\bar{\beta}_1}{\beta_2}$, where $\bar{\beta}_1$ and $\bar{\beta}_2$ take the same sign. Next we consider the value of $\eta_2 = 1$. Substituting the value of τ, we have

$$\frac{\tau\beta_1\bar{\beta}_2{}^2}{\bar{\beta}_2} = \beta_1\bar{\beta}_1\left(\frac{\bar{\beta}_1}{\bar{\beta}_2}\right)^2 = 1,$$

which gives

$$\left(\frac{\bar{\beta}_1}{\bar{\beta}_2}\right)^2 = \frac{1}{\beta_1\bar{\beta}_1}.$$

Finally, we have $\rho = \tau\beta_2\bar{\beta}_1 = 1$, so

$$\rho = \frac{\bar{\beta}_1}{\bar{\beta}_2}\bar{\beta}_1\beta_2\frac{\bar{\beta}_2}{\bar{\beta}_2} = \beta_2\bar{\beta}_2\left(\frac{\bar{\beta}_1}{\bar{\beta}_2}\right)^2 = \frac{\beta_2\bar{\beta}_2}{\beta_1\bar{\beta}_1} = 1.$$

This implies that β_1 and β_2 attain the same sign. Generalizing, one can find that $\rho = \pm 1$ if $\beta_2\bar{\beta}_2\left(\frac{\bar{\beta}_1}{\bar{\beta}_2}\right)^2 = \pm 1$. Hence the topologically equivalent form of system (5.5) takes the form

$$\frac{dw_1}{dt} = w_2 \tag{5.6a}$$

$$\frac{dw_2}{dt} = w_1^2 + \rho w_1 w_2, \text{ where } \rho = \pm 1. \tag{5.6b}$$

Since $\beta_1\beta_2 \neq 0$, we can determine the values of $\bar{\beta}_1$ and $\bar{\beta}_2$ with the help of the above process so that $\rho = \pm 1$. Therefore, a versal deformation candidate of the system (5.6) can easily be written as

$$\frac{dw_1}{dt} = w_2 \tag{5.7a}$$

$$\frac{dw_2}{dt} = \epsilon_1 + \epsilon_2 w_2 + w_1^2 + \rho w_1 w_2, \tag{5.7b}$$

where ϵ_1 and ϵ_2 are the unfolding deformation parameters. Since the non-degeneracy condition $\beta_1\beta_2 \neq 0$ is satisfied, system (2.2) has a cusp bifurcation of codimension 2 in a neighborhood of the unique coexistence equilibrium point (x^*, y^*).

6. Numerical simulations

In this section, we perform numerical simulations to validate our analytical findings in the previous sections. We consider the following parametric values for the strong additive Allee effect: K = 2, $\delta = 0.1$, r = 0.28, n = 0.08, h = 0.01, m = 0.017, a = 0.03 and $e = 0.3$. Default values of all the parameters are given in Table 2.

Since the predator and prey nullclines do not intersect in the feasible region for very low (i.e., $d < 0.0035$) or very high (i.e., $d > 0.00503$) mortality rates of the predator species, both species do not coexist in that situation. However, for moderate predator mortality rates ($0.0035 < d < 0.00503$), both species can coexist. Therefore, in the intermediate values of the mortality rate, we have the following cases: (i) The predator and prey species do not coexist (Fig. 1(a)). (ii) The two nullclines intersect at three points: $E_3^{1*} = (1.0073, 7.9246)$, $E_3^{2*} = (0.6526, 6.7962)$, and $E_3^{3*} = ((0.3400, 3.8517))$ for $d = 0.00446$ (Fig. 1(b)). Both species survive in a coexistence steady state

Table 2 Description of the system parameters in the model system (2.2) and their dimensions (M stands for mass and T for time).

Parameters	Value	Description	Dimensions
x	–	Prey size	M
y	–	Predator size	M
r	0.280	Intrinsic prey growth rate	$1/T$
K	2.000	Environmental intake capacity	M
n	0.080	Survival threshold of prey	M
m	0.017	Predator's consumption rate	$1/T$
δ	0.100	Prey refuge coefficient	$1/M$
a	0.030	Half saturation constant	M
d	–	Natural death rate of predator	$1/T$
e	0.300	Conversion factor	(dimensionless)
h	0.010	Auxiliary parameter	M

E_3^{1*}, but the other two equilibrium points E_3^{2*} and E_3^{3*} are saddles (Fig. 3(a)–(b)). (iii) Increasing the value of d slightly to 0.004495, both predator and prey nullclines intersect at $E_2^{1*} = (1.0372, 7.8491)$ and touch each other at $E_2^{2*} = (0.4813, 5.3650)$ (Fig. 1(c)). In this case, we get the second equilibrium point by collapsing E_3^{2*} and E_3^{3*}. The dynamical system is asymptotically stable at the equilibrium point E_2^{1*}, since both eigenvalues of the Jacobian matrix at the equilibrium point E_2^{1*} are negative. On the other hand, the coincident point $E_2^{2*} = (0.4813, 5.3650)$ is a saddle, so the dynamical system is not stable for the low density of the species (Fig. 3(c)–(d)). (*iv*) Two nontrivial nullclines intersect at the unique equilibrium point $E_1^* = (1.1235, 7.5433)$ for the predator mortality rate $d = 0.00460$ (Fig. 1(d)). The eigenvalues of the unique equilibrium point $E_1^* = (1.1235, 7.5433)$ are $(-0.002144, -0.044075)$, so the dynamical system is asymptotically stable at the equilibrium point $E_3^{1*} = (1.0073, 7.9246)$, and both species survive in a coexistence steady state (Fig. 3 (e)–(f)).

Using parameters $K = 2$, r = 0.28, n = 0.08, h = 0.01, m = 0.017, a = 0.03, e = 0.3 and $d = 0.0042$, the dynamical system (2.2) experiences a saddle-node bifurcation around the interior equilibrium point $(0.9153, 8.3456)$. Using Sotomayor's theorem [37], $v_2^T[F_\delta(E^*, \delta_{sn})] = -8.597730990 \neq 0$ and $v_2^T[D^2F(E^*, \delta_{sn})(v_1, v_1)] = 0.1335001295 \neq 0$; hence, from these transversality conditions, system (2.2) undergoes a non-degenerate saddle-node bifurcation of co-dimension one around the interior equilibrium point $E^* = (0.9153, 8.3456)$ when the refuge coefficient δ passes through its threshold value $\delta = \delta_{sn} = 0.1015$. The behaviour is periodic around the coexistence equilibrium point $(0.9520, 7.6637)$ for the predator mortality value $d = 0.00460$ and for the threshold value of the refuge coefficient $\delta = \delta_{hb} = 0.0927$ (Fig. 2), with the remaining parameters as in Table 2. Note that the first Lyapunov number is $\eta = 484.6445$, so the Hopf bifurcation is subcritical.

The possible equilibria and the nature of the dynamical system at all the equilibria are summarised in Table 3. Below the threshold of the refuge coefficient δ, both predator and prey

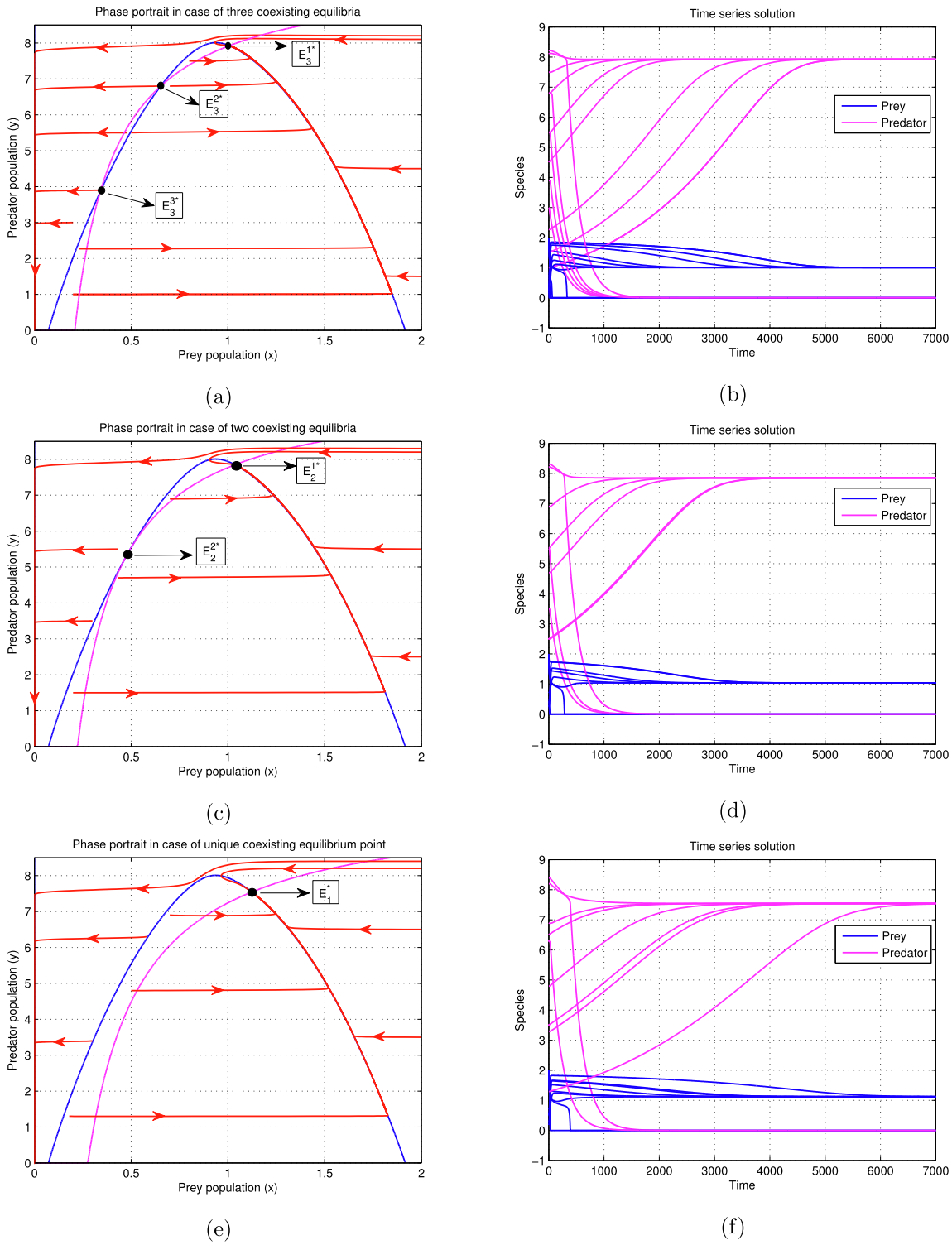

Fig. 3 Phase portrait depicting local stability when system (2.2) has (a)–(b) three coexisting equilibria, of which E_3^{1*} is stable and E_3^{2*} and E_3^{3*} are unstable for $d = 0.00446$; (c)–(d) two coexisting equilibria, of which E_2^{1*} is stable and E_2^{2*} is unstable for $d = 0.004495$; and (e)–(f) only one equilibrium point E_1^*, which is stable for $d = 0.0046$. All other parameters are given in Table 2.

species will go extinct. They coexist mutually in an ecosystem when the refuge coefficient δ passes through its threshold δ_{hb} (see Fig. 4 and Table 4). Similarly, fixing $\delta_{hb} = 0.0927$, the Allee parameter $n = 0.08$; setting other parameters as in Table 2, both the species coexist in an oscillating mode. Just above the threshold value of the Allee parameter, both species go extinct, but below the threshold they coexist (see Fig. 5 and Table 5).

Consider the Bogdanov–Takens parameters (r, δ), and set the other parameters to be $K = 2$, a = 0.14, m = 0.25, e = 0.27,

Table 3 Schematic representation of the nature of system (2.2) about the interior equilibrium point (remaining parametric default values are given in Table 2): LAS = locally asymptotically stable, US = unstable, HB = Hopf bifurcation, SN = saddle-node bifurcation, MP = multiple point.

Equilibria	d	δ	Solution	Eigenvalues	Nature
E_1^*	0.00460	0.1	(1.1235,7.5433)	(−0.0021, −0.044)	LAS
E_1^*	0.00420	0.1015	(0.9153, 8.3456)	(0.00045, −0.0036)	SN
E_1^*	0.00460	0.0927,	(0.9520, 7.6637)	(0±0.0064i)	HB
E_2^{1*}	0.004495	0.1	(1.0372, 7.8492)	(−0.0036, −0.0224)	LAS
$E_2^{2*}(MP)$	0.004495	0.1	(0.4813, 5.3650)	(0.1239, 0.00001)	US
E_3^{1*}	0.00446	0.1	(1.0073, 7.9246)	(−0.004987, −0.0141)	LAS
E_3^{2*}	0.00446	0.1	(0.6526, 6.7962)	(0.0765, −0.00037)	US
E_3^{3*}	0.00446	0.1	(0.3400, 3.8517)	(0.1613, 0.00019)	US

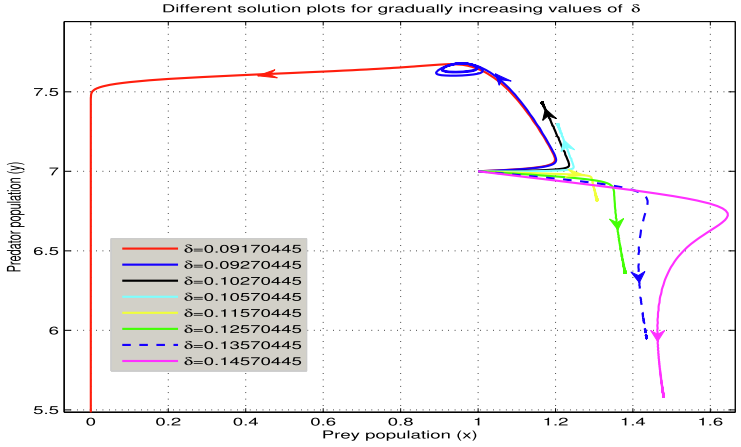

Fig. 4 Phase trajectories for increasing values of δ. All other parameters are as in Table 2.

Table 4 Different equilibrium positions according to gradual increment of the refuge coefficient δ, where $n = 0.08$ and other parameters are given in Table 2.

δ	(x^*, y^*)	Fig. 4
0.0917	(0,0)	Red
0.0927	(0.9537,7.6651)	Blue
0.1027	(1.1657,7.4313)	Black
0.1057	(1.2058,7.2949)	Cyan
0.1157	(1.3074,6.8181)	Yellow
0.1257	(1.3797,6.3638)	Green
0.1357	(1.4350,5.9517)	Dashed blue
0.1457	(1.4792,5.5826)	Magenta

d = 0.125, n = 0.02 and $h = 0.011$. Both eigenvalues of the Jacobian matrix evaluated at the coexistence equilibrium point $(1.0944, 1.8239)$ are zero for the critical values $(r_{bt}, \delta_{bt}) = (1.7749, 0.7007)$. The canonical form of system (2.2) also satisfies the non-degeneracy condition $\beta_1\beta_2 \neq 0$. Therefore, the dynamical system (2.2) experiences a Bogdanov–Takens bifurcation [35,47] in the neighborhood of the coexistence equilibrium point $(x^*, y^*) = (1.0944, 1.8239)$. Fig. 6 depicts phase portraits of the Bogdanov–Takens bifurcation for different perturbations of the Bogdanov pair (r, δ). For an illustrative example, consider system (2.2) with the strong additive Allee effect on the prey population only and a Holling type II predator response function in the form

$$\frac{dx}{dt} = rx\left(1 - \frac{x}{K} - \frac{n}{x+h}\right) - \frac{mx(1-\delta y)y}{a + x(1-\delta y)} = F_1, \tag{6.1a}$$

$$\frac{dy}{dt} = \left(\frac{emx(1-\delta y)}{a + x(1-\delta y)} - d\right)y = F_2. \tag{6.1b}$$

Set the numerical values of the biological constants to be K = 2, a = 0.14, m = 0.25, e = 0.27, d = 0.125, n = 0.02, h = 0.011, $\delta = 0.7007$ and $r = 1.7749$. We can rewrite system (6.1) as follows:

$$\frac{dx}{dt} = 1.7749x\left(1 - \frac{x}{2} - \frac{0.02}{(x+0.011)}\right) - 0.25\frac{xy(-0.7007y+1)}{0.14 + x(-0.7007y+1)}, \tag{6.2a}$$

$$\frac{dy}{dt} = \left(0.0675\frac{x(-0.7007y+1)}{0.14 + x(-0.7007y+1)} - 0.125\right)y. \tag{6.2b}$$

System (6.2) has a coexistence equilibrium point $(1.0944, 1.8239)$, where both the eigenvalues of the variational matrix are zero. By making a simple transformation $x = (1.0944 + x_1)$, $y = (1.8239 + y_1)$ and expanding Eq. (6.2) with the Taylor series, the equation takes the form

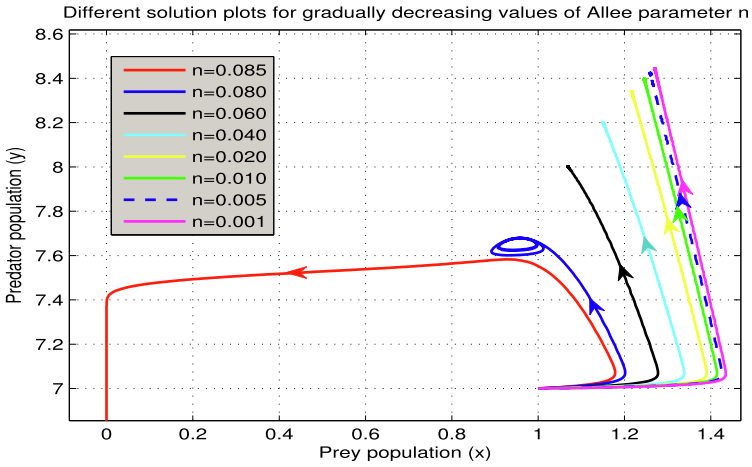

Fig. 5 Phase trajectories for decreasing values of the Allee parameter n. All other parameters are in Table 2.

Table 5 Different equilibrium positions according to gradual reduction of the Allee parameter n, where $\delta = 0.0927$ and other parameters are given in Table 2.

n	(x^*, y^*)	Fig. 5
0.085	(0,0)	Red
0.080	(0.9537, 7.6651)	Blue
0.060	(1.0689, 8.0016)	Black
0.040	(1.1506, 8.1993)	Cyan
0.020	(1.2166, 8.3398)	Yellow
0.010	(1.2459, 8.3973)	Green
0.005	(1.2598, 8.4237)	Dashed blue
0.001	(1.2706, 8.4438)	Magenta

$$\frac{dx_1}{dt} = 0.4894x_1 + 1.3496x_2 - 1.9993x_1^2 - 4.1174x_1x_2 - 7.4640x_2^2 + O(\|x\|^3), \quad (6.3a)$$

$$\frac{dx_2}{dt} = -0.1775x_1 - 0.4894x_2 + 0.3003x_1^2 + 1.1117x_1x_2 + 2.0153x_2^2 + O(\|x\|^3). \quad (6.3b)$$

Taking another transformation

$$y_1 = x_1,$$
$$y_2 = 0.4894x_1 + 1.3496x_2,$$

Eqs. (6.3) transform to

$$\frac{dy_1}{dt} = y_2 - 1.4877y_1^2 + 0.9602y_1y_2 - 4.0982y_2^2 + O(\|y\|^3), \quad (6.4a)$$

$$\frac{dy_2}{dt} = -3.6127y_1^2 + 0.1200y_1y_2 - 0.5123y_2^2 + O(\|y\|^3). \quad (6.4b)$$

Applying the C^∞ invertible transformation,

$$z_1 = y_1 + 0.5102y_1^2 + 4.0982y_1y_2,$$
$$z_2 = y_2 - 0.9561y_1y_2 - 1.4877y_1^2,$$

Eq. (6.4) reduces to

$$\frac{dz_1}{dt} = z_2 + O(\|z\|^3), \quad (6.5a)$$

$$\frac{dz_2}{dt} = -3.6127z_1^2 - 2.8554z_1z_2 + O(\|z\|^3). \quad (6.5b)$$

Applying a further transformation

$$w_1 = z_1,$$
$$w_2 = z_2 + O(\|z\|^3),$$

Eq. (6.5) transforms to

$$\frac{dw_1}{dt} = w_2, \quad (6.6a)$$

$$\frac{dw_2}{dt} = -3.6127w_1^2 - 2.8554w_1w_2 + O(\|w\|^3). \quad (6.6b)$$

7. Conclusion

We introduced an additive prey Allee effect to our previous predator–prey model [17] (the previous model is identical to system (2.1) with $n = 0$), discussed the dynamical behaviour of the system at different equilibrium points and determined the stability of equilibrium points for an additive Allee effect. Then we identified all possible local and global bifurcations in order to get insight into the dynamics of the model. The Bogdanov–Takens bifurcation is identified numerically. The refuge coefficient δ and Allee parameter n are very sensitive and have a stabilizing effect in the system. For the threshold value of the refuge parameter $\delta_{hb} = 0.0927$, the model undergoes a Hopf bifurcation around the unique positive equilibrium and exhibits a stable limit cycle, meaning the predator and prey can coexist in an oscillating manner around the positive equilibrium. The refuge coefficient is more sensitive than our previous study, where the nature of the Hopf bifurcation was supercritical; in the present study, it is subcritical. From a mathematical and empirical point of view, we have seen that just below the threshold value of the refuge coefficient, both species go extinct (Fig. 4)), and the dynamical system breaks down. In our previous study, we observed that decreasing the refuge coefficient from its critical level caused both species to coexist in an oscillating fashion. We also observed that the prey species have more protection for the gradually increasing value of the refuge coefficient. The prey volume increases and leads to prey population outbreak; on the other hand, the predator population decreases. Availability of food decreases for high refuge values, and that reduces the predator population, which ultimately goes to extinction after a long time (Fig. 4). Table 4

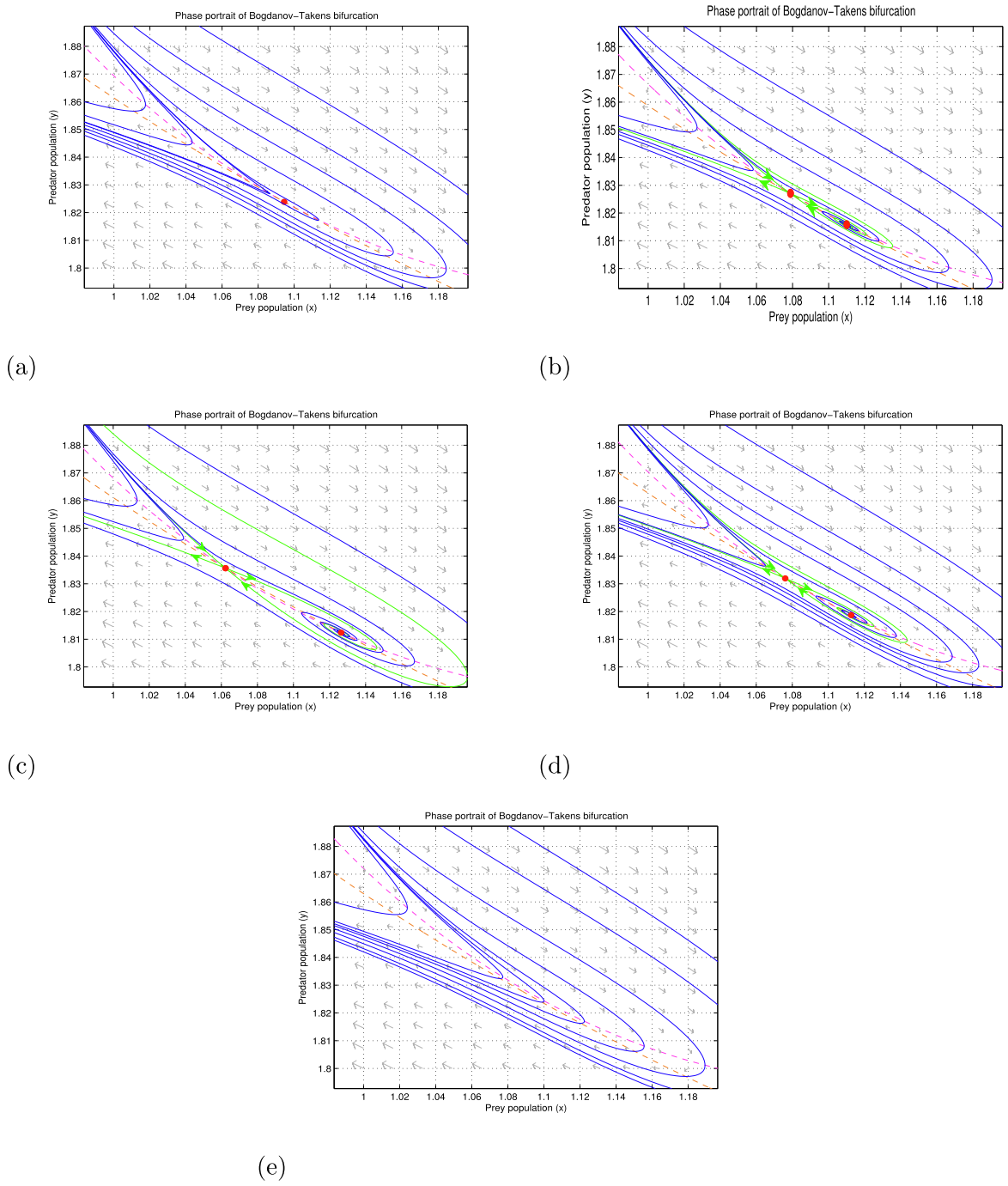

Fig. 6 Phase portrait of the Bogdanov–Takens bifurcation of system (2.2) in the neighborhood of the equilibrium point $(x^*, y^*) = (1.0944, 1.8239)$. The threshold values of the Bogdanov–Takens parameters are $(r_{hb}, \delta_{bt}) = (1.7749, 0.7007)$. For a small perturbation, (a) $r_1 = 0, \delta_1 = 0$, (b) $r_2 = -0.002, \delta_2 = 0.001$, (c) $r_3 = 0.002, \delta_3 = 0.0001$, (d) $r_4 = 0.002, \delta_4 = -0.0005$ and $r_5 = -0.001, \delta_5 = -0.0006$. The other parameter values are $K = 2$, a = 0.14, m = 0.25, e = 0.27, d = 0.125, n = 0.02 and $h = 0.011$.

indicates that the predator volume decreases and the prey volume increases at the same time, enhancing the rate of convergence to the coexistence equilibrium according to increment of the refuge coefficient δ.

For the critical values $\delta_{hb} = 0.0927$ and $n = 0.08$, the dynamical system is periodic. If the value of the Allee parameter n is greater than that of the threshold value, predator and prey both go extinct. Fig. 5 depicts that, for the gradual decrease of the Allee parameter n from its threshold value $n = 0.08$, the dynamical system changes from its oscillatory mode to a stable mode, and the volume of both species increases. Therefore, it can be reported that both predator and prey species coexist for smaller values than the threshold value. Hence, we conclude that, for the joint presence of prey

refuge and strong additive Allee effect, both species coexist in an ecological system for a long time.

Modelling a natural ecosystem is much more complex than modelling any interacting population in a laboratory. Hence, ecological systems should be modelled as open systems with environmental fluctuations [14]. On the other hand, delay and diffusion are also important in population dynamics [30–32]. To this end, in future work, we will extend our system subject to the above effects, which could generate spatial heterogeneity in terms of spatiotemporal patterns. We will also incorporate the effects of delay due to growth and migration of both predator and prey.

Compliance with Ethical Standards

SRS? is supported by NSERC Discovery and Horizons Grants.

Declaration of Competing Interest

The authors declare that they have no known competing financial interests or personal relationships that could have appeared to influence the work reported in this paper.

Acknowledgment

SS is grateful to the Department of Mathematics & Statistics, Aliah University, for providing opportunities to perform the present work. For citation purposes, please note that the question mark in "Smith?" is part of her name.

Appendix A.

A.1. Jacobian

The Jacobian matrix for the model system (2.2) at the interior equilibrium point is given by

$$J^* = \begin{bmatrix} rx^*\left(\frac{1}{K}+\frac{n}{(x^*+h)^2}\right)+\frac{d^2y^*}{e^2mx^*} & \frac{\delta\, dy^*}{e(-\delta y^*+1)}-\frac{d}{e}-\frac{\delta\, d^2y^*}{e^2m(-\delta y^*+1)} \\ \left(\frac{d}{x^*}-\frac{d^2}{emx^*}\right)y^* & \left(-\frac{\delta\, d}{-\delta y^*+1}+\frac{\delta\, d^2}{emx^*(-\delta y^*+1)}\right)y^* \end{bmatrix}.$$

A.2. δ_j values

The values of $\delta_1, \delta_2, \delta_3$ are given by

$$\begin{aligned}
\delta_1 = {} & Ke^3m^2nrx^{*3}-e^3h^2m^2rx^{*3}-2e^3hm^2rx^{*4}-e^3m^2rx^{*5}+2Kde^2h^2m^2x^*y^* \\
& +4Kde^2hm^2x^{*2}y^*+2Kde^2m^2x^{*3}y^*-2Kd^2eh^2mx^*y^*-4Kd^2ehmx^{*2}y^* \\
& -2Kd^2emx^{*3}y^*-Kde^2mnrx^{*2}+de^2h^2mrx^{*2}+2de^2hmrx^{*3}+de^2mrx^{*4} \\
& +Kd^3h^2x^*y^*+2Kd^3hx^{*2}y^*+Kd^3x^{*3}y^*-Kd^3h^2y^*-2Kd^3hx^*y^*-Kd^3x^{*2}y^*, \\
\delta_2 = {} & -Ke^2mnrx^{*2}+e^2h^2mrx^{*2}+2e^2hmrx^{*3}+e^2mrx^{*4}-Kd^2h^2y^*-2Kd^2hx^*y^* \\
& -Kd^2x^{*2}y^*, \\
\delta_3 = {} & y^*\big(-Kde^2h^2mx^*-2Kde^2hmx^{*2}-Kde^2mx^{*3}-Ke^2mnrx^{*2}+e^2h^2mrx^{*2} \\
& +2e^2hmrx^{*3}+e^2mrx^{*4}+Kd^2eh^2+2Kd^2ehx^*+Kd^2ex^{*2}-Kd^2h^2y^* \\
& -2Kd^2hx^*y^*-Kd^2x^{*2}y^*\big).
\end{aligned}$$

A.3. p_{ij} coefficients

The values of the differential coefficient p_{ij}, where $i,j=0,1,2,3$, are as follows:

$$\begin{aligned}
p_{10} = {} & r\left(1-\frac{x^*}{K}-\frac{n}{x^*+h}\right)+rx^*\left(-\frac{1}{K}+\frac{n}{(x^*+h)^2}\right)+\frac{m(\delta y^*-1)y^*}{-\delta x^*y^*+a+x^*} \\
& +\frac{mx^*(\delta y^*-1)^2y^*}{(-\delta x^*y^*+a+x^*)^2}, \\
p_{01} = {} & \frac{mx^*\left(-\delta^2x^{*2}y^{*2}+2\delta y^*a+2\delta x^*y^*-a-x^*\right)}{(-\delta x^*y^*+a+x^*)^2}, \\
p_{12} = {} & =\frac{\delta a((\delta y^*-1)x^{*2}+2ax^*y^*\delta+a^2)m}{(-\delta x^*y^*+a+x^*)^4}, \\
p_{21} = {} & \frac{m(\delta y^*-1)a(3\delta y^*a+\delta x^*y^*-a-x^*)}{(-\delta x^*y^*+a+x^*)^4}, \\
p_{20} = {} & \frac{\left(-(x^*+h)^2+nK\right)r}{K(x^*+h)^2}-\frac{rx^*n}{(x^*+h)^3}+\frac{m(\delta y^*-1)^2y^*}{(-\delta x^*y^*+a+x^*)^2}+\frac{mx^*(\delta y^*-1)^3y^*}{(-\delta x^*y^*+a+x^*)^3}, \\
p_{11} = {} & \frac{ma(2\delta y^*a+\delta x^*y^*-a-x^*)}{(-\delta x^*y^*+a+x^*)^3}, \\
p_{30} = {} & -1/2\,\frac{rn}{(x^*+h)^3}+1/2\,\frac{rx^*n}{(x^*+h)^4}-1/2\,\frac{m(-\delta y^*+1)^3y^*}{(-\delta x^*y^*+a+x^*)^3}+1/2\,\frac{m(\delta y^*-1)^4x^*y^*}{(\delta x^*y^*-a-x^*)^4} \\
q_{10} = {} & -\frac{em(\delta y^*-1)ay^*}{(-\delta x^*y^*+a+x^*)^2}, \\
q_{01} = {} & \frac{-(\delta y^*-1)^2(-em+d)x^{*2}+2a(y^*(-em+d)\delta+1/2em-d)x^*-a^2d}{(-\delta x^*y^*+a+x^*)^2}, \\
q_{12} = {} & \frac{m\delta\left(x^{*2}y^{*2}\delta^2+3ax^*y^*\delta-y^*\delta x^{*2}+a^2-ax^*\right)}{(-\delta x^*y^*+a+x^*)^3}, \\
q_{21} = {} & \frac{(3\delta y^*a+\delta x^*y^*-a-x^*)a(\delta y^*-1)m}{(-\delta x^*y^*+a+x^*)^4}, \\
q_{20} = {} & -\frac{em(\delta y^*-1)^2ay^*}{(-\delta x^*y^*+a+x^*)^3}, \\
q_{11} = {} & \frac{ma(2\delta y^*a+\delta x^*y^*-a-x^*)}{(-\delta x^*y^*+a+x^*)^3}, \\
q_{03} = {} & -\frac{em\delta^2x^{*2}a(a+x^*)}{(-\delta x^*y^*+a+x^*)^4}.
\end{aligned}$$

A.4. c_{ij} and d_{ij} values

The detailed expressions of c_{ij} and d_{ij} $(i,j=0,1,2)$ of system (5.1) are given as follows:

$$\begin{aligned}
c_{10} = {} & r\left(1-\frac{x^*}{K}-\frac{n}{x^*+h}\right)+rx^*\left(-\frac{1}{K}+\frac{n}{(x^*+h)^2}\right)-\frac{m(-\delta y^*+1)y^*}{-\delta x^*y^*+a+x^*} \\
& +\frac{m(-\delta x^*y^*+x^*)y^*(-\delta y^*+1)}{(-\delta x^*y^*+a+x^*)^2}, \\
c_{01} = {} & \frac{m\delta x^*y^*}{-\delta x^*y^*+a+x^*}-\frac{m(-\delta x^*y^*+x^*)}{-\delta x^*y^*+a+x^*}-\frac{m(-\delta x^*y^*+x^*)y^*\delta x^*}{(-\delta x^*y^*+a+x^*)^2} \\
c_{11} = {} & r\left(-\frac{1}{K}+\frac{n}{(x^*+h)^2}\right)-\frac{rx^*n}{(x^*+h)^3}+\frac{m(-\delta y^*+1)^2y^*}{(-\delta x^*y^*+a+x^*)^2} \\
& -\frac{m(-\delta x^*y^*+x^*)y^*(-\delta y^*+1)^2}{(-\delta x^*y^*+a+x^*)^3}, \\
c_{12} = {} & \frac{m\delta y^*}{-\delta x^*y^*+a+x^*}-2\,\frac{m\delta x^*y^*(-\delta y^*+1)}{(-\delta x^*y^*+a+x^*)^2}-\frac{m(-\delta y^*+1)}{-\delta x^*y^*+a+x^*} \\
& +\frac{m(-\delta x^*y^*+x^*)(-\delta y^*+1)}{(-\delta x^*y^*+a+x^*)^2}-\frac{m(-\delta x^*y^*+x^*)y^*\delta}{(-\delta x^*y^*+a+x^*)^2} \\
& +2\,\frac{m(-\delta x^*y^*+x^*)y^*\delta x^*(-\delta y^*+1)}{(-\delta x^*y^*+a+x^*)^3}, \\
c_{22} = {} & \frac{m\delta x^*}{-\delta x^*y^*+a+x^*}+\frac{m\delta^2x^{*2}y^*}{(-\delta x^*y^*+a+x^*)^2} \\
& -\frac{m(-\delta x^*y^*+x^*)\delta x^*}{(-\delta x^*y^*+a+x^*)^2}-\frac{m(-\delta x^*y^*+x^*)y^*\delta^2x^{*2}}{(-\delta x^*y^*+a+x^*)^3}, \\
d_{10} = {} & \left(\frac{em(-\delta y^*+1)}{-\delta x^*y^*+a+x^*}-\frac{em(-\delta x^*y^*+x^*)(-\delta y^*+1)}{(-\delta x^*y^*+a+x^*)^2}\right)y^*,
\end{aligned}$$

$$d_{01}=\left(-\frac{em\delta x^*}{-\delta x^*y^*+a+x^*}+\frac{em(-\delta x^*y^*+x^*)\delta x^*}{(-\delta x^*y^*+a+x^*)^2}\right)y^*+\frac{em(-\delta x^*y^*+x^*)}{-\delta x^*y^*+a+x^*}-d,$$

$$d_{11}=\left(-\frac{em(-\delta y^*+1)^2}{(-\delta x^*y^*+a+x^*)^2}+\frac{em(-\delta x^*y^*+x^*)(-\delta y^*+1)^2}{(-\delta x^*y^*+a+x^*)^3}\right)y^*,$$

$$d_{12}=\left(-\frac{em\delta}{-\delta x^*y^*+a+x^*}+2\frac{em\delta x^*(-\delta y^*+1)}{(-\delta x^*y^*+a+x^*)^2}+\frac{em(-\delta x^*y^*+x^*)\delta}{(-\delta x^*y^*+a+x^*)^2}\right.$$
$$\left.-2\frac{em(-\delta x^*y^*+x^*)\delta x^*(-\delta y^*+1)}{(-\delta x^*y^*+a+x^*)^3}\right)y^*+\frac{em(-\delta y^*+1)}{-\delta x^*y^*+a+x^*}$$
$$-\frac{em(-\delta x^*y^*+x^*)(-\delta y^*+1)}{(-\delta x^*y^*+a+x^*)^2},$$

$$d_{22}=\left(\frac{em\delta^2x^{*2}}{(-\delta x^*y^*+a+x^*)^2}+\frac{em(-\delta x^*y^*+x^*)\delta^2x^{*2}}{(-\delta x^*y^*+a+x^*)^3}\right)y^*-\frac{em\delta x^*}{-\delta x^*y^*+a+x^*}$$
$$+\frac{em(-\delta x^*y^*+x^*)\delta x^*}{(-\delta x^*y^*+a+x^*)^2}.$$

References

[1] J. Banerjee, S.K. Sasmal, R.K. Layek, Supercritical and subcritical Hopf-bifurcations in a two-delayed prey-predator system with density-dependent mortality of predator and strong Allee effect in prey, Bios. 180 (2019) 19–37.

[2] G. Birkhoff, G.C. Rota, Ordinary differential equations, Wiley, New York, 1978.

[3] W.C. Allee, Animal aggregations, A Study in General Sociology, University of Chicago Press, 1931.

[4] Y. Cai, C. Zhao, W. Wang, J. Wang, Dynamics of Leslie-Gower predator–prey Model With Additive Allee Effect, Appl. Math. Model. 39 (2015) 2092–2106.

[5] L. Chen, F. Chen, L. Chen, Regulation and stability of host-parasite population interactions: I. Regulatory processes, Qualitative analysis of a predator–prey model with Holling type II functional response incorporating a constant prey refuge, Non. Anals: Real World Appls. 11 (2010) 246–252.

[6] E. González-Olivares, J. Cabrera-Villegas, F. Córdova-Lepe, A. Rojas-Palma, Competition among Predators and Allee Effect on Prey, Their Influence on a Gause-Type Predation Model, Math. Prob. Engg. (2019).

[7] E.D. González-Olivares, B. Gonzalez-Yanez, J. Mena-Lorca, R. Ramos-Jiliberto, Modelling the Allee effect: are the different mathematical forms proposed equivalents, in: R. Mondaini (Ed.), Proceedings of the International Symposium on Mathematical and Computational Biology BIOMAT 2006, 2006, pp. 53–71.

[8] M.M. Haque, S. Sarwardi, Dynamics of a harvested predator–prey model with prey refuge dependent on both species, I.J.B.C 28(12) (2018) 1830040.

[9] M.P. Hassell, The dynamics of arthropod predator–prey systems, Princeton University Press, Princeton, NJ, 1978.

[10] C.S. Holling, The components of predation as revealed by a study of small-mammal predation of the european pine sawfly, The Canadian Entomologist, Cambridge Univ Press 91 (1959) 293–320.

[11] C.S. Holling, The functional response of predator to prey density and its role in mimicry and population regulations, Mem. Entomol. Soc. Canada 97 (1965) 5–60.

[12] T.K. Kar, Stability analysis of a predator–prey model incorporating a prey refuge, Commun. Nonlinear Sci. Numer. Simul. 10 (2005) 681–691.

[13] A.J. Lotka, Elements of mathematical biology, Dover Publication, New York, 1956.

[14] L. Li, Z. Jin, Pattern dynamics of a spatial predator–prey model with noise, Nonl. Dyn. 67 (2012) 1737–1744.

[15] S.J. Majeed, R.K. Naji, A.A. Thirthar, The dynamics of an Omnivore-predator–prey model with harvesting and two different nonlinear functional responses, AIP Publishing 2096 (1) (2019).

[16] N. Min, M. Wang, Hopf bifurcation and steady-state bifurcation for a Leslie-Gower predator–prey model with strong Allee effect in prey, Discrete Continu. Dyn. Syst. A 39 (2) (2019) 1071–1099.

[17] H. Molla, Md.S. Rahman, S. Sarwardi, Dynamics of a predator–prey Model with Holling Type II Functional Response Incorporating a Prey Refuge Depending on Both the Species, IJNSNS 20 (2019) 1–16.

[18] D. Mukherjee, The effect of refuge and immigration in a predator–prey system in the presence of a competitor for the prey, Nonlin. Anal.: Real World Appl. 31 (2016) 277–287.

[19] H.T. Odum, W.C. Allee, A note on the stable point of populations showing both intraspecific cooperation and disoperation, Ecology 35 (1954).

[20] P.J. Pal, P.K. Mandal, Bifurcation analysis of a modified Leslie-Gower predator–prey model with Beddington–DeAngelis functional response and strong Allee effect, Math. Comp. Sim. 97 (2014) 123–146.

[21] S. Pal, S. Majhi, S. Mandal, Role of fear in a predator–prey model with Beddington–DeAngelis functional response, Z. Naturforsch. A 74 (2019) 581–595.

[22] S. Pal, N. Pal, J. Chattopadhyay, Hunting cooperation in a discrete-time predator–prey system, IJBC 28 (2018).

[23] L. Perko, Differential equations and dynamical systems, Springer, New York, 2001.

[24] F.A. Rihan, H.J. Alsakaji, Persistence and extinction for stochastic delay differential model of prey predator system with hunting cooperation in predators, Adv. Differ. Eqs. 2020 (1) (2020) 1–22.

[25] F.A. Rihan, H.J. Alsakaji, C. Rajivganthi, Stability and Hopf bifurcation of three-species prey-predator System with time delays and Allee Effect, Complexity (2020) Article ID 7306412.

[26] W. Rudin, Principles of Mathematical Analysis (International Series in Pure & Applied Mathematics), Mc-Hill, New York, 1976.

[27] S. Saha, A. Maiti, G.P. Samanta, A Michaelis-Menten predator–prey model with strong Allee effect and disease in prey incorporating prey refuge, Int. J. Bifurc. Chaos 28 (6) (2018).

[28] S. Sarwardi, P.K. Mandal, S. Ray, Analysis of a competitive prey-predator system with a prey refuge, Bios. 110 (3) (2012) 133–148.

[29] S.K. Sasmal, Population dynamics with multiple Allee effects induced by fear factors–A mathematical study on prey-predator interactions, Appl. Math. Model. 64 (2018) 1–14.

[30] S. Sarwardi, M. Haque, P.K. Mandal, Ratio-dependent predator–prey model of interacting population with delay effect, Nonl. Dyn. 69 (2012) 817–836.

[31] S. Sarwardi, M. Haque, P.K. Mandal, Persistence and global stability of Bazykin predator–prey model with Beddington–DeAngelis response function, Commun. Nonl. Sci. Numer. Simulat. 19 (2014) 189–209.

[32] S. Sarwardi, Md.M. Haque, S. Hossain, Analysis of Bogdanov-Takens bifurcations in a spatiotemporal harvested-predator and prey system with Beddington–DeAngelis type response function, Nonl. Dyn. 100 (2020) 1755–1778.

[33] M. Sen, M. Banerjee, Y. Takeuchi, Influence of Allee effect in prey populations on the dynamics of two-prey-one-predator model, Math. Biosci. Eng. 15 (4) (2018) 883–904.

[34] D. Sen, S. Ghorai, M. Banerjee, Allee Effect in Prey versus Hunting Cooperation on Predator-Enhancement of Stable Coexistence, IJBC 29 (6) (2019).

[35] A. Sha, S. Samanta, M. Martcheva, Backward bifurcation, oscillations and chaos in an eco-epidemiological model with fear effect, J. Biol. Dyn. 13 (2019) 301–327.

[36] X. Song, Y. Li, Dynamic behaviors of the periodic predator–prey model with modified Leslie-Gower Holling-type II schemes and impulsive effect, Non. Anal.: Real World Appls. 9 (2008) 64–79.
[37] J. Sotomayor, Generic bifurcations of dynamical systems, Dyn. Sys. 54 (1973) 560–950.
[38] A.M. Teixeira, F.M. Hilker, Hunting cooperation and Allee effects in predators, J. Theor. Biol. 419 (2017) 13–22.
[39] M. Verma, A.K. Misra, Modeling the effect of prey refuge on a ratio-dependent predator–prey system with the Allee effect, Bull. Math. Biol. 80 (3) (2018) 626–656.
[40] V. Volterra, La concorrenza vitale tra le specie nell'ambiente marino, Soc. nouv. de l'impr. du Loiret (1931).
[41] X. Wang, L.Y. Zanette, X. Zou, Modelling the fear effect in predator–prey interactions, J. Math. Biol. 73 (2016) 1179–1204.
[42] S. Wiggins, Introduction to Applied Nonlinear Dynamical Systems and Chaos, Springer-Verlag, USA, 1991.
[43] Z. Xiao, X. Xie, Y. Xue, Stability and bifurcation in a Holling type II predator–prey model with Allee effect and time delay, Adv. Diff. Equ. 1 (2018).
[44] S. Xu, Dynamics of a general predator–prey model with prey-stage structure and diffusive effects, Comput. Math. Appl. 68 (3) (2014) 405–423.
[45] Y. Yong, L. Hua, W. Yu-mei, Ming Ma, K. Zhang, Dynamic Study of a predator–prey Model with Weak Allee Effect and Delay, Adv. Math. Phys. (2019).
[46] T. Yu, Y. Tian, H. Guo, X. Song, Dynamical analysis of an integrated pest management predator–prey model with weak Allee effect, J. Biol. Dyn. (2019) 1–27.
[47] L. Zhang, C. Zhang, He Zhirong, Codimension-one and codimension-two bifurcations of a discrete predator–prey system with strong Allee effect, Math. Comp. Sim. 162 (2019) 155–178.